B-cell clusters at the invasive margin associate with longer survival in early-stage oral-tongue cancer patients

Phanthunane, C.; Wijers, R.; Herdt, M. de; Langeveld, T.P.M.; Koljenovic, S.; Dasgupta, S.; ... ; Debets, R.

OncoImmunology

ISSN: (Print) (Online) Journal homepage: https://www.tandfonline.com/loi/koni20

B-cell clusters at the invasive margin associate with longer survival in early-stage oral-tongue cancer patients

C. Phanthunane, R. Wijers, M. de Herdt, T.P.M. Langeveld, S. Koljenovic, S. Dasgupta, S. Sleijfer, R. J. Baatenburg de Jong, J. Hardillo, H. E. Balcioglu & R. Debets

To cite this article: C. Phanthunane, R. Wijers, M. de Herdt, T.P.M. Langeveld, S. Koljenovic, S. Dasgupta, S. Sleijfer, R. J. Baatenburg de Jong, J. Hardillo, H. E. Balcioglu & R. Debets (2021) B-cell clusters at the invasive margin associate with longer survival in early-stage oral-tongue cancer patients, OncoImmunology, 10:1, 1882743, DOI: 10.1080/2162402X.2021.1882743

To link to this article: https://doi.org/10.1080/2162402X.2021.1882743

ONCOIMMUNOLOGY
2021, VOL. 10, NO. 1, e1882743 (11 pages)
https://doi.org/10.1080/2162402X.2021.1882743

Taylor & Francis
Taylor & Francis Group

ORIGINAL RESEARCH

OPEN ACCESS Check for updates

B-cell clusters at the invasive margin associate with longer survival in early-stage oral-tongue cancer patients

C. Phanthunane[a,b], R. Wijers[c], M. de Herdt[a], T.P.M. Langeveld[d], S. Koljenovic[a], S. Dasgupta[a], S. Sleijfer[c], R. J. Baatenburg de Jong[a], J. Hardillo[a], H. E. Balcioglu[c*], and R. Debets[c*]

[a]Departments of Otorhinolaryngology and Erasmus MC Cancer Institute, Rotterdam, The Netherlands; [b]Department of Medical Oncology, HRH Princess Chulabhorn College of Medical Science, Bangkok, Thailand; [c]Departments of Medical Oncology, Erasmus MC Cancer Institute, Rotterdam, The Netherlands; [d]Department of Otorhinolaryngology, Head and Neck Surgery, Leiden University Medical Center, Leiden, The Netherlands

ABSTRACT

In oral-cancer, the number of tumor-infiltrating lymphocytes (TILs) associates with improved survival, yet the prognostic value of the cellular composition and localization of TILs is not defined. We quantified densities, localizations, and cellular networks of lymphocyte populations in 138 patients with T1-T2 primary oral-tongue squamous cell carcinoma treated with surgical resections without any perioperative (chemo)radiotherapy, and correlated outcomes to overall survival (OS). Multiplexed in-situ immunofluorescence was performed for DAPI, CD4, CD8, CD20, and pan-cytokeratin using formalin-fixed paraffin-embedded sections, and spatial distributions of lymphocyte populations were assessed in the tumor and stroma compartments at the invasive margin (IM) as well as the center of tumors. We observed a high density of CD4, CD8, and CD20 cells in the stroma compartment at the IM, but neither lymphocyte densities nor networks as single parameters associated with OS. In contrast, assessment of two contextual parameters within the stroma IM region of tumors, i.e., the number of CD20 cells within 20 µm radii of CD20 and CD4 cells, termed the *CD20 Cluster Score*, yielded a highly significant association with OS (HR 0.38; $p = .003$). Notably, the *CD20 Cluster Score* significantly correlated with better OS and disease-free survival in multivariate analysis (HR 0.34 and 0.47; $p = .001$ and 0.019) as well as with lower local recurrence rate (OR: 0.13; $p = .028$). Taken together, our study showed that the presence of stromal B-cell clusters at IM, in the co-presence of CD4 T-cells, associates with good prognosis in early oral-tongue cancer patients.

ARTICLE HISTORY
Received 9 October 2020
Revised 13 January 2021
Accepted 25 January 2021

KEYWORDS
Multiplex in situ staining; tissue contexture of lymphocytes; T-cell; B-cell; tongue cancer; survival; immune micro-environment

Introduction

Oral cavity squamous cell carcinoma (OSCC), the most common type of head and neck cancer (HNC), annually accounts for more than 350,000 new cases and 170,000 deaths worldwide.[1] Early-stage OSCC patients are mainly treated with radical surgery, followed by adjuvant radiotherapy or chemoradiotherapy in those cases with unfavorable histopathologic features, such as nodal metastasis, extra nodal extension, inadequate surgical margin, perineural invasion, and lymphovascular invasion.[2] Despite the general success of surgery in early-stage OSCC patients, approximately 20% of these patients die within 5 years.[3,4] To identify early-stage OSCC patients with short survival, and select treatments for this patient subgroup, there is a need for an easy-to-determine, robust and quantitative prognostic marker.

In-situ characterization of the tumor microenvironment (TME) facilitates the identification of parameters associated with survival and responsiveness to therapy,[5–7] where type, density and location of tumor-infiltrating lymphocytes (TILs) have been reported to be predictive of cancer patient survival.[8] In general, high CD8 T-cell numbers at the tumor center and invasive margin (IM) associate with favorable prognosis in various cancers.[9] CD4 and CD8 T-cells have been the main focus of multiple studies that interrogate the prognostic value of TILs, however, recent studies have shown that also CD20 B-cells contribute to anti-tumor activities, such as production of antibodies, acting as antigen-presenting cells and interaction with other immune cells, as well as release of pro-inflammatory molecules.[10–13]

A number of studies has assessed the prognostic value of lymphocyte numbers in OSCC, mostly in advanced stage, and demonstrated that densities of CD4, CD8, and CD20 cells are associated with survival.[14–16] In contrast, in early-stage OSCC patients, the cellular composition and tissue localization of TILs, and their putative roles in anti-tumor responses, remains largely unknown. In this study, we interrogated the contexture of CD4, CD8, and CD20 lymphocytes using multispectral imaging and digital quantification to discover its association with survival in early-stage (T_{1-2}, N_{0-1}) oral-tongue cancer, the most common subsite for OSCC, in a cohort of 138 patients. Our findings demonstrated that the presence of stromal clusters of B-cells together with CD4 T-cells at IM, which yields the so-called *CD20 Cluster Score*, acts as a strong independent prognostic factor in early-stage oral-tongue cancer.

CONTACT H. E. Balcioglu h.balcioglu@erasmusmc.nl Departments of Medical Oncology, Erasmus MC Cancer Institute, Rotterdam, The Netherlands.
*joint senior authors

Supplemental data for this article can be accessed on the publisher's website.

Materials and methods

Study population

We retrospectively reviewed medical database of patients with pathological T1-2 oral-tongue cancer who received treatment at Leiden University Medical Center between July 2000 and October 2010 (LUMC; Leiden, The Netherlands, n = 47) and Erasmus Medical Center between October 2007 and December 2015 (EMC; Rotterdam, The Netherlands, n = 91). Informed consent was obtained from all 138 patients. All patients had histologically proven primary oral-tongue cancer and underwent curative surgery without any perioperative treatment. Relevant clinical history, pathological staging according to UICC 7th edition, and at least 3-year follow-up were documented. HPV status was not documented. Human tissues and patient data were used according to "The Code of Conduct for Responsible Use" and "The Code of Conduct for Health Research" as stated by the Federation of Dutch Medical Scientific Societies (http://www.federa.org/). Furthermore, The Erasmus MC Medical Ethics Committee approved the research protocol (MEC-2016-751).

Histopathological analysis

Formalin-fixed paraffin-embedded (FFPE) tissue blocks and Hematoxylin and eosin (H&E) stained glass slides of the included patients were retrieved from the archives. H&E stained sections were digitally scanned for high-resolution whole slide images (WSI). Histological parameters, namely, differentiated grading, vascular invasion, perineural invasion, and depth of invasion (DOI) were reviewed by pathologists using the glass slides or WSI.

Immunofluorescence staining

Immunofluorescence (IF) in-situ staining was performed with the Opal™ 4-tumor lymphocyte kit (OP4LY1001KT, PerkinElmer, Waltham, MA, USA) consisting of CD4, CD8, CD20, and pan-Cytokeratin (CK) antibodies and DAPI. Staining was performed on 4 µm FFPE sections according to the manufacturer's guidelines. In brief, 4 sequential rounds of staining were performed; each round including: antigen retrieval with microwave treatment in buffer; blocking; primary antibody incubation; secondary antibody incubation; and subsequent incubation with tyramide signal amplification (TSA) plus fluorophore,[17] with washing steps in between. Finally, sections were counterstained with spectral DAPI and mounted with Vectrashield fluorescent mounting medium (Vector Laboratories, Burlingame, CA, USA). Details of the five-color multiplex protocol are provided in **Table S1.**

Multispectral imaging and analysis

Multiplex stained sections were imaged using the Vectra Multispectral Imaging System version 3.0 (Akoya, Menlo Park, CA, USA). First, whole sections were scanned using low magnification (4x; **Figure S1A**) to select regions of interest (ROIs), and these ROIs were scanned to acquire multispectral images using high magnification (20x; **Figure S1, C and G**). Selection of ROIs was performed in the center (C, 8 stamps) or the IM of the tumor (8 stamps). In case of very small tumors, at least 4 stamps were set per region. Stamps at tumor center were placed between tumor margin and basement, and those at IM were placed at tumor margin. Tumor basement was defined as CK positive area interrupting basement membrane (exemplified by green line in Figure S1A), and tumor margin was defined as the outermost part of the CK positive area reaching into the stroma (exemplified by white line in Figure S1A). Both C and IM stamps were selected where CK positive and negative regions were present. Positioning of stamps was verified with corresponding H&E sections to exclude non-cancer, in-situ cancer, and salivary structures (**Figure S1B**). Multispectral images were 0.356 mm^2 (690.4 µm x 515.8 µm) in size and analyzed with trainable algorithms using the inForm® software version 2.0 (Akoya). Images were spectrally unmixed using signatures of individual fluorophores corresponding to the markers of interest and corrected for autofluorescence, and subjected to tissue segmentation, cell segmentation and cell phenotyping. Algorithm training for tissue segmentation was performed by selecting tumor and stroma compartments based on CK and DAPI signals (Figures S1D and H): tumor segment (CK-positive, DAPI-positive); stroma segment (CK-negative, DAPI-positive); and non-tissue segment (CK-negative, DAPI-negative) for 8 individual stamps from 20 patients. Stamping and segmentation yielded 4 distinct regions, namely: center tumor (C-T); center stroma (C-S); IM tumor (IM-T); and IM stroma (IM-S). Training of the software for detection and phenotyping of individual cells was again performed for 8 individual stamps from 20 patients, based on fluorescent expression patterns and cell morphology (**Figure S1E and I**). The cellular phenotypes of interest were: CD4 T helper cell (CD4+, Th), CD8 cytotoxic T-cell (CD8+), CD20 B-cell (CD20+), cancer cell (CK+) and others (**Figure S1E and I**). The stamping and generation of trainable algorithms were performed blinded to clinical information.

Densities and cellular networks

Densities of lymphocytes were calculated per stamp, averaged over the stamps for one of 4 regions per patient and reported as cells/mm^2. Spatial relationships between cell types with certain phenotypes were studied using the center of cells and according to Nearest Neighbor Analysis (NNA), which included distances (in µm) from one cell type to the nearest other cell type (i.e., CD20toCD4); and the number of one cell type within 20 µm of the same or another cell type (i.e., CD20WCD20). Due to the relative scarcity of lymphocytes in tumor compartments, all NNA was performed in stroma compartments. NNA was performed with the R-studio software version 1.0.153 (RStudio Inc., Boston, MA, USA) with the following packages; tidyverse, ggplot2, and phenoptr (Akoya).

CD20 cluster score

The *CD20 Cluster Score* captures the parameters number of CD20 cells within 20 µm of CD4 cells (CD20WCD4) and number of CD20 cells within 20 µm of other CD20 cells (CD20WCD20) at

the IM-S region. The two individual parameters were classified into high versus low using its respective median value as a cutoff, after which the two parameters were combined into a single ordinal variable yielding either a high (CD20WCD4 high and CD20WCD20 high) or low score (CD20WCD4 low and CD20WCD20 low; CD20WCD4 high and CD20WCD20 low; or CD20WCD4 low and CD20WCD20 high).

Scoring Tertiary lymphoid structure (TLS)

TLS quantification was performed in 10 selected patients with either high or low CD 20 Cluster Score (5 patients from each group). In these tissues, we manually counted TLS structures, where each TLS consisted of lymphocyte-rich areas (either CD4, CD8 or CD20 cells) and peripheral node addressin-positive high-endothelial venules (PNAd+ HEVs). Single staining of PNAd (MECA-79, BioLegend, San Diego, CA, USA, diluted 1:25) was performed using standard immunohistochemistry process as previously described.[18] Quantification was performed using high power magnification (20x) scanned images. HEVs were defined as endothelial cells of which more than a single cell stained positive for PNAd.[19]

Statistical analysis

Patients were randomly split into discovery (n = 69) and validation (n = 69) cohorts with no significant difference based on clinicopathological characteristics (listed in Table S2) or lymphocyte densities. Overall survival (OS) was defined as the time from diagnosis to death from any cause; disease-free survival (DFS) as the time after primary resection to time of recurrence or death; and time to recurrence (TTR) as the time after primary resection to time of first recurrence. Survival times were plotted using Kaplan-Meier survival curves and significant differences were assessed by log-rank tests. Cox proportional hazard regression models using the enter method were used to determine univariate hazard ratios, and variables with p-values <0.2 were subsequently used for multivariate Cox modeling using the backward elimination likelihood ratio method. Odds ratios were used for TTR analysis. Categorical variables were presented by frequency and percentages, and continuous variables were presented by median or mean values. Comparisons between categorical variables were performed by Chi-square test, and comparisons between categorical and continuous variables were performed by Wilcoxon-signed rank test or Mann-Whitney U for dependent or independent samples, respectively. Correlations between continuous variables were evaluated using Spearman rank correlation test. All significant differences were tested two-sided, and p-values < 0.05 were considered statistically significant. Statistical analyses were performed using SPSS 24.0 software (SPSS Inc. Chicago, IL, USA).

Results

Preferential localization of CD20 B-cells in stroma invasive margin in early tongue cancer

Cells were identified either as CD4, CD8, CD20, cancer or other cells in the tumor or stroma compartments, each subdivided into center or IM regions (**Figure S1**). Quantification of lymphocyte densities in the discovery cohort of 69 patients with pathological T1-2 oral-tongue cancer (see **Table S2**) showed higher abundance of all lymphocyte subsets in the stroma when compared to the tumor compartment, and at IM when compared to center regions of the tumor, resulting in the highest lymphocyte density at IM-S, and the lowest lymphocyte density at C-T (Figure 1b-d). Higher density of CD20 cells at IM-T was significantly associated with longer OS in the discovery cohort (Figure 1g: HR 0.26; 95% CI 0.10–0.67; p = 0.003). No significant prognostic value was observed for densities of CD4 or CD8 cells at C-T, C-S, IM-T, and IM-S and also not for CD20 cells at C-T, C-S, and IM-S (Kaplan-Meier survival curves for lymphocyte density at IM-T and IM-S are summarized in Figure 1e-j).

We then focused on those regions of tumors with sufficient cell numbers for analysis of cellular networks of lymphocytes and their association with OS. To this end, we calculated nearest distances between cells (Figure 2b **to D**) and numbers of cells within 20 µm radius of cells (figure 2f **to H**) at IM-S. In the discovery cohort, we observed significantly longer OS for patients with high numbers of CD20 cells within 20 µm radius of other CD20 cells (i.e., high CD20WCD20; Figure 2n: HR 0.40; 95% CI 0.17–0.96; p = 0.034), and high CD20WCD4 and CD20WCD8 showed trends for an association with longer OS (Figure 2l **and M**: HR 0.50, 95% CI 0.22–1.18; p = 0.107, and HR: 0.49; 95% CI 0.21–1.15; p = 0.095, respectively). Notably, CD20WCD20 strongly correlated with CD20 cell density at IM-S (Spearman correlation coefficient 0.67; p < 0.001) but not IM-T. In order to further assess the prognostic value of these single contextual parameters, we tested our findings from the discovery cohort in a separate validation cohort (69 patients). In the validation cohort, neither the density of CD20 cells nor the CD20WCD20 were statistically significant for OS (analysis for the discovery and the validation cohorts are summarized in Table 1).

The *CD20 Cluster Score*, a measure of the proximity of CD20 cells to CD4 and CD20 cells, correlates with patient survival

To study the relevance of the presence and clustering of B cells in relation to patient survival, clearly present in the total cohort of 138 patients, we assessed the prognostic value of different combinations of single contextual parameters at IM-S. Along this line, we combined two parameters at a time, focusing on density and networks of CD20 cells (survival associated with CD20-centered combinational parameters for CD4-CD20 and CD8-CD20 in the discovery and the validation cohort is shown in Table 2). In the discovery cohort, the combination of high CD4 and CD20 densities showed a significant adverse association with OS, whereas

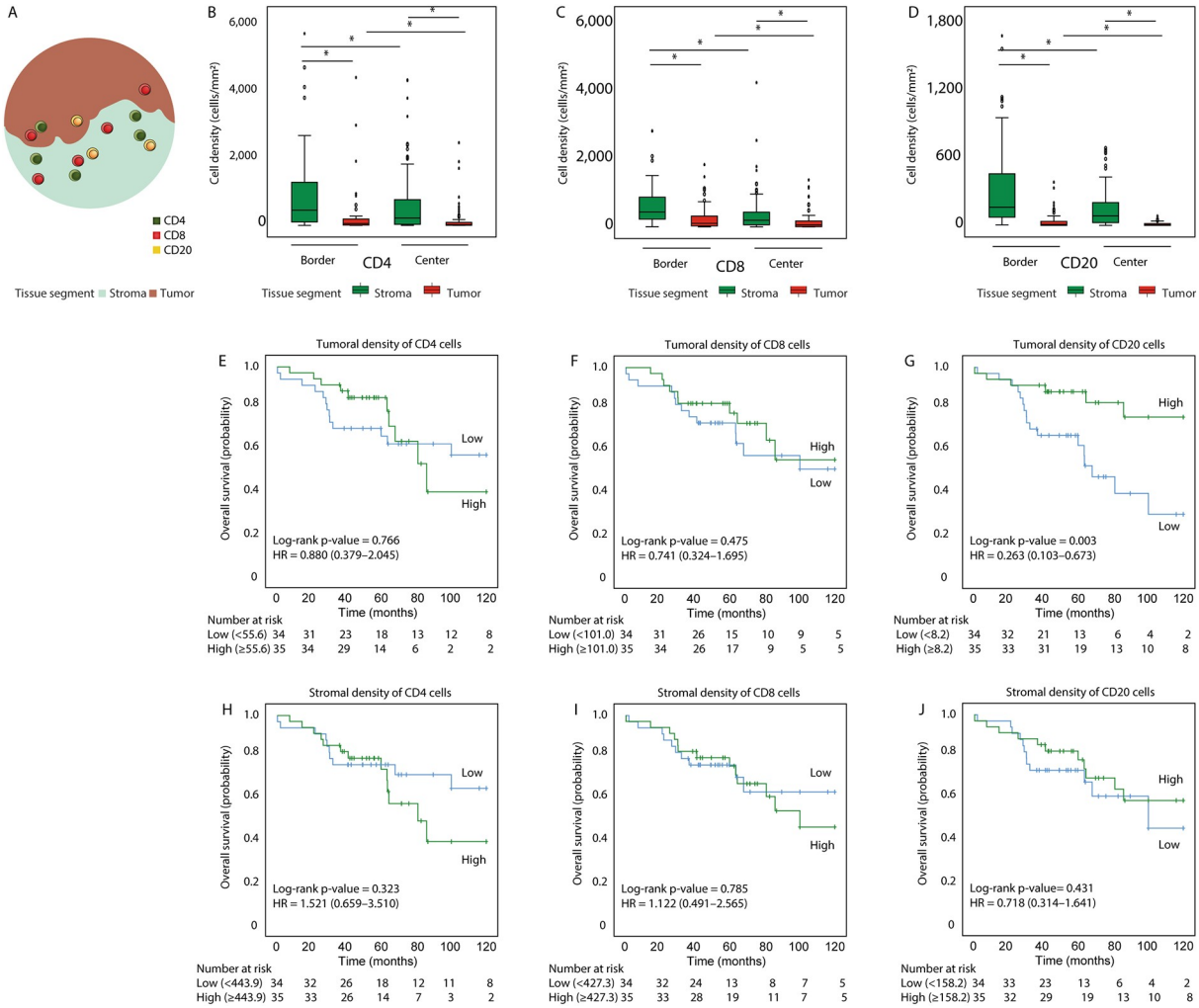

Figure 1. Tumoral density of CD20 cells, but not CD4 and CD8 cells, associates with OS in the discovery cohort.(A) Cartoon depicting lymphocyte phenotyping and tissue segmentation (stroma and tumor). (**B-D**) Box plots showing (**B**) CD4, (**C**) CD8 and (**D**) CD20 lymphocyte densities in tumor and stroma IM and center regions. (**E-J**) Overall survival analyses according to either tumoral or stromal densities of (**E** and **H**) CD4, (**F** and **I**) CD8 or (**G** and **J**) CD20 lymphocytes in the IM region, where low and high values were stratified using median density as a cutoff. Data is shown for the discovery cohort (n = 69 patients). Statistical significance was tested using the (**B-D**) Wilcoxon signed-rank test or (**E-J**) log-rank test. *: p-value < 0.05. p-values and hazard ratios (HR with 95% confidence interval (CI) in parentheses) are listed within the graphs with numbers below graph listing median cutoff and number of patients at risk.

the combination of high CD20WCD4 and CD20WCD20 numbers showed a significant beneficial association with OS (Table 2, p = 0.013 and 0.044, respectively). In contrast, none of the tested combinations of CD8 and CD20 parameters were significant in the discovery cohort. In the validation cohort, only the combination of CD20WCD4 and CD20WCD20 upheld statistical significance (Table 2, p = 0.026) yet not the combination of CD4 and CD20 densities (Table 2, p = 0.339).

Next, we used the combination of CD20WCD4 and CD20WCD20, from here on referred to as the "*CD20 Cluster Score*" (detailed in Materials and Methods). Multiplex images of tumors with high *CD20 Cluster Scores* showed that both B-cells and T-cells are present in the same clusters at IM-S region (Figure 3a **to D**). The *CD20 Cluster Score* high patients had significantly longer OS in the discovery (Figure 3e, HR 0.34; 95% CI 0.14–0.84; p = 0.015), validation (figure 3f, HR: 0.42; 95% CI 0.18–0.99; p = 0.042), as well as the total patient cohort (HR 0.034; 95% CI 0.20–0.71; p = 0.002). Interestingly, subgroup analysis revealed that the favorable prognostic value of the *CD20 Cluster Score* is particularly evident in cases with low density of CD4 cells at IM-S (Figure 4a, HR: 0.25; 95% CI 0.08–0.76; p = 0.015). Indeed, density of CD4 cells at IM-S negatively correlated with CD20WCD20 (**Figure S2**; correlation coefficient = −0.58, p < 0.001). Interestingly, when comparing the occurrence of TLS according to the co-presence of lymphocytes and HEVs, we observed a significantly higher TLS count in patients with a high *CD20 Cluster Score* (**Figure S3**; median number 3 vs 0, respectively, p-value 0.043). Collectively, our findings point out that the presence of clusters containing CD20 B-cells and CD4 T-cells (as measured by the number of CD20 cells within a 20 µm radius of CD20 and CD4 cells) rather than the mere densities of these

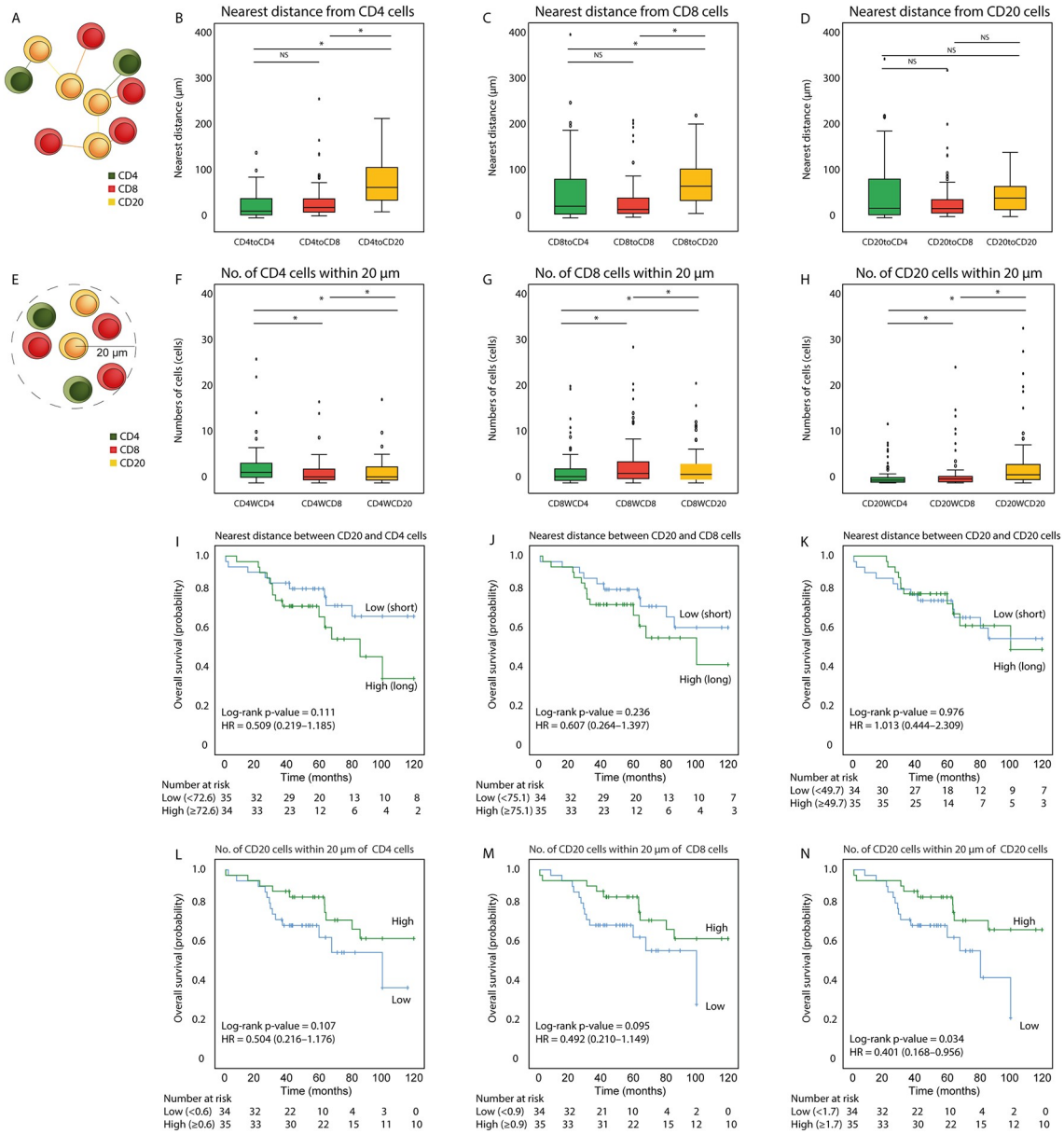

Figure 2. Clustering of stromal CD20 cells in stroma IM region of tumor associates with OS in the discovery cohort. (**A, E**) cartoons depicting cellular network parameters; (**A**) nearest neighbor distances and (**E**) number of cells within 20 µm radius. (**B-D** and **F-H**) Boxplots showing nearest neighbor analysis (NNA) of lymphocytes. Nearest distances from (**B**) CD4, (**C**) CD8 and (**D**) CD20 lymphocytes to other lymphocytes; and numbers of (**F**) CD4, (**G**) CD8 and (**H**) CD20 lymphocytes within 20 µm of other CD4, CD8 or CD20 lymphocytes. (**I-N**) Overall survival analyses according to NNA parameters of CD20 cells in IM-S region, where low and high values were stratified using median NNA values as a cutoff. Nearest distances between CD20 cells and either (**I**) CD4, (**J**) CD8 or (**K**) CD20 cells; and numbers of CD20 cells within a 20 µm radius of either (**L**) CD4, (**M**) CD8 or (**N**) CD20 cells. Data is shown for the discovery cohort (n = 69 patients). Statistical significance was tested using the (**B-D** and **F-H**) Wilcoxon signed-rank and (**I-N**) log-rank test. *: *p*-value < 0.05. *p*-values and HR with 95% CI (in parentheses) are listed within the graphs and numbers below graph listing median cutoff and number of patients at risk.

cells provide prognostic value, and that the prognostic value is most pronounced in cases where densities of CD4 T-cells are low (Figure 4b).

The *CD20 cluster score* positively correlates with OS and DFS in multivariate analysis

Assessing the prognostic value of the *CD20 Cluster Score* together with the clinicopathological outcomes of our patient cohort (Table 3) using univariate analysis demonstrated that patients with a high *CD20 Cluster Score* or of age <65 years had a longer OS (HR: 0.38; 95% CI 0.20–0.71; $p = 0.003$; HR 3.28, 95% CI 1.79–6.04; $p < 0.001$). Multivariate analysis demonstrated that the high *CD20 Cluster Score* was significantly predictive of a longer OS when adjusted for patient's age, perineural invasion and locoregional recurrence status (HR: 0.34; 95% CI 0.18–0.65; $p = 0.001$). Further assessment of the *CD20 Cluster Score* in a subgroup of patients that were staged according to 8th AJCC/UICC (90 patients) indicated that the CD20 Cluster Score was still predictive for OS in multivariate analysis (**Table S3**, HR: 0.13; 95% CI 0.02–1.00; $p = 0.050$).

In addition to OS, we also assessed the value of the *CD20 Cluster Score* toward DFS and tumor recurrence rates.

Table 1. OS analysis for single contextual parameters in the discovery and validation cohorts [a.]

	Discovery cohort (n = 69)				Validation cohort (n = 69)			
	Estimated mean survival (months)		HR (95% CI)	p-value	Estimated mean survival (months)		HR (95% CI)	p-value
Parameter	Low	High			Low	High		
Tumoral density of CD4	85.6	86.0	0.880 (0.379–2.045)	0.767	83.8	77.7	1.017 (0.453–2.286)	0.967
Tumoral density of CD8	84.3	91.6	0.741 (0.324–1.695)	0.477	90.1	80.4	1.480 (0.675–3.245)	0.327
Tumoral density of CD20	72.9	102.8	0.263 (0.103–0.673)	0.005	83.4	86.5	0.800 (0.369–1.731)	0.570
Stromal density of CD4	93.0	81.5	1.521 (0.659–3.510)	0.326	86.6	74.2	1.330 (0.585–3.025)	0.497
Stromal density of CD8	89.8	87.2	1.122 (0.491–2.565)	0.785	86.6	84.6	1.086 (0.499–2.364)	0.835
Stromal density of CD20	84.9	91.5	0.718 (0.314–1.641)	0.433	80.7	88.6	0.668 (0.303–1.470)	0.315
Nearest distance between CD20 and CD4	95.2	79.6	0.509 (0.219–1.185)	0.117	88.2	78.4	0.676 (0.304–1.505)	0.337
Nearest distance between CD20 and CD8	93.8	82.0	0.607 (0.264–1.397))	0.241	75.4	94.8	2.135 (0.950–4.798)	0.067
Nearest distance between CD20 and CD20	87.0	89.4	1.013 (0.444–2.309)	0.976	84.9	81.0	0.860 (0.388–1.905)	0.710
Number of CD20 within 20 μm radius of CD4	78.3	95.3	0.504 (0.216–1.176)	0.113	82.6	87.9	0.814 (0.372–1.781)	0.606
Number of CD20 within 20 μm radius of CD8	72.6	95.3	0.492 (0.210–1.149)	0.101	84.3	81.1	1.317 (0.571–3.039)	0.518
Number of CD20 within 20 μm radius of CD20	69.9	97.0	0.401 (0.168–0.956)	0.039	70.1	90.1	0.546 (0.239–1.249)	0.152

[a]Table lists OS analyses of estimated mean OS, HR, 95% CI, and *p*-value in the discovery and validation cohorts.

Table 2. Combination of two contextual parameter of CD20 and CD4 cells associates with OS [a.]

		Discovery cohort (*n* = 69)			Validation cohort (*n* = 69)		
Combination analysis	Group	*n*	Estimated mean survival (months)	p-value	*n*	Estimated mean survival (months)	p-value
CD4 and CD20							
Stromal density of CD4 and CD20	LoLo	18	74.2	0.013	15	78.6	0.399
	HiLo	16	99.7		19	76.5	
	LoHi	16	112.5		19	92.8	
	HiHi	19	73.4		19	70.0	
CD20toCD4 and CD20toCD20	LoLo	30	91.5	0.706	10	69.0	0.725
	HiLo	4	NA		24	86.4	
	LoHi	5	NA		22	78.1	
	HiHi	30	84.3		13	79.4	
CD20WCD4 and CD20WCD20	LoLo	30	73.7	0.044	24	78.2	0.026
	HiLo	4	49.4		10	54.6	
	LoHi	4	66.5		10	69.4	
	HiHi	31	100.6		25	98.8	
CD8 and CD20							
Stromal density of CD8 and CD20	LoLo	24	81.0	0.665	20	88.7	0.364
	HiLo	10	78.8		14	61.4	
	LoHi	10	100.4		14	87.0	
	HiHi	25	86.9		21	92.2	
CD20toCD8 and CD20toCD20	LoLo	31	91.7	0.771	20	82.9	0.927
	HiLo	3	NA		14	87.4	
	LoHi	3	NA		14	68.2	
	HiHi	32	86.2		21	82.7	
CD20WCD8 and CD20WCD20	LoLo	31	72.1	0.167	30	75.7	0.007
	HiLo	3	66.0		4	42.3	
	LoHi	3	70.3		4	NA	
	HiHi	32	97.8		31	83.1	

[a]List of all CD20-centered parameters assessed for their association with survival. Log-rank *p*-value was tested and listed. Mean survival time was estimated by Kaplan-Meier survival curve.

Abbreviations: CD20toCD4, nearest distances between CD20 and CD4; CD20toCD8, nearest distances between CD20 and CD8; CD20toCD20, nearest distances between CD20 and CD20; CD20WCD4, numbers of CD20 within 20 μm of CD4; CD20WCD8, numbers of CD20 within 20 μm of CD8; CD20WCD20, numbers of CD20 within 20 μm of CD20.

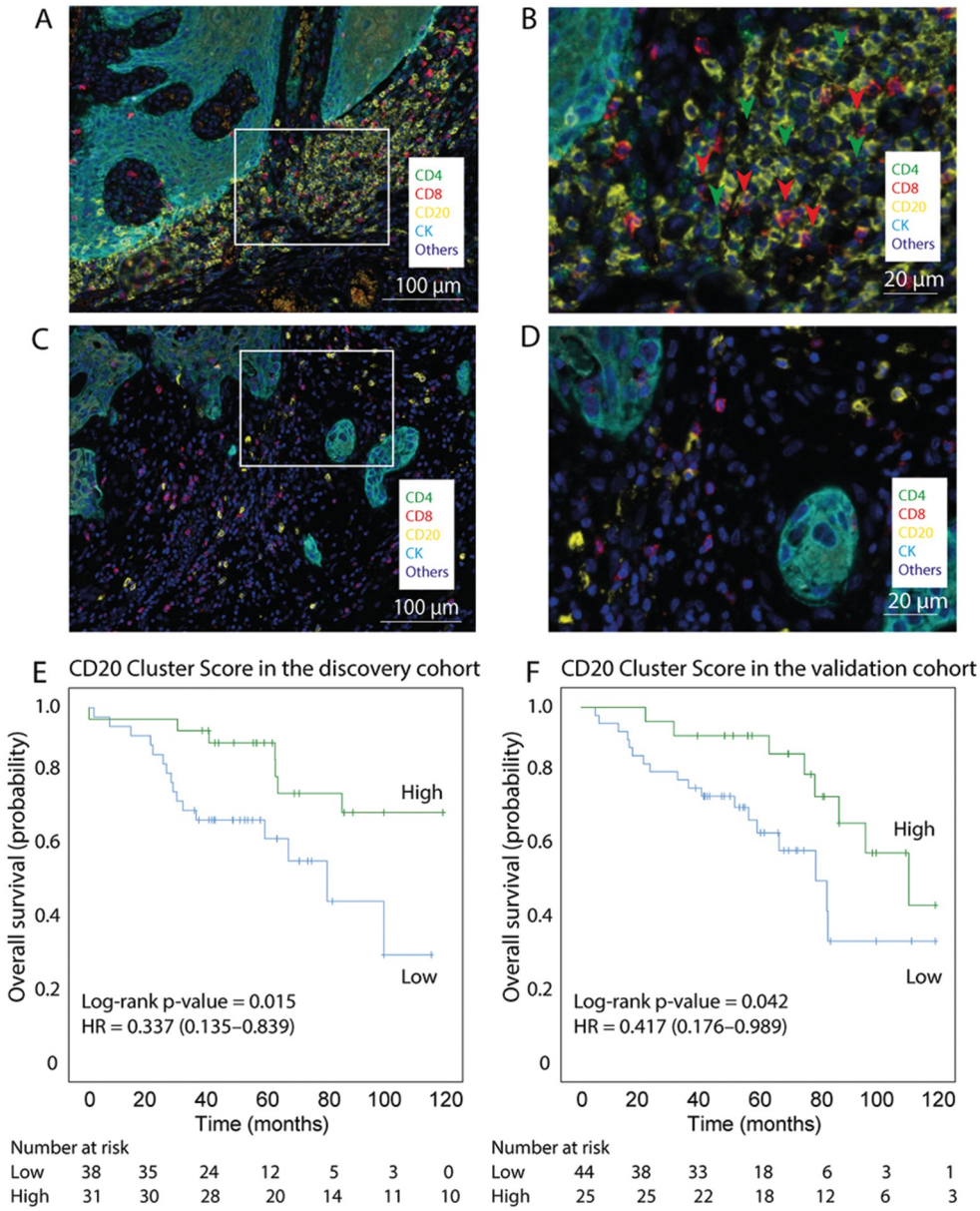

Figure 3. Numbers of stromal CD20 cells within the vicinity of CD20 as well as CD4 cells in IM-S region are associated with OS. (**A-F**) Representative multiplex images of oral-tongue cancer tissue (**A, C**, magnification 20x; **B, D**, zoomed in) of a *CD20 Cluster Score* (**A, B**) High and (**C, D**) Low patient. (**B**) High density of stromal CD20 cells in close vicinity of CD4 (green arrowhead) and CD8 cells (red arrowhead). (**D**) Low density of stromal CD20 cells accompanied by low density of CD4 and CD8 cells. (**E, F**) Overall survival analyses of *CD20 Cluster Score* in the discovery cohort (**E**, $n = 69$) and in the validation cohort (**F**, $n = 69$). Log-rank p-values and HR with 95% CI (in parentheses) are listed within the graphs (**E, F**) with numbers below graph listing number of patients at risk (**E, F**).

Consistent with OS, the 5-year DFS was improved in both univariate and perineural invasion adjusted multivariate analysis (**Table S4**, HR: 0.46; 95% CI 0.24–0.87; $p = 0.017$, and HR: 0.47; 95% CI 0.25–0.88; $p = 0.019$, respectively). Interestingly, local recurrence rate, but not regional nor locoregional recurrence rates, was significantly lower in patients with a high *CD20 Cluster Score* (**Table S5**, OR: 0.13; 95% CI 0.02–1.00; $p = 0.028$). The median time to local recurrence was longer, however not significant, in patients with a high versus low *CD20 Cluster Score* (40.0 vs 9.4 months, respectively).

Discussion

In this study, using multiplex in situ immunofluorescence and computational image analyses of 138 patients with T1-T2 primary oral-tongue squamous cell carcinoma, we observed a high density of CD20 cells that clustered together in the IM-S regions. Notably, we introduced the *CD20 Cluster Score*, a score which combines the number of CD20 cells within 20 µm radii of CD20 as well as CD4 cells, which yielded significant associations with OS, DFS and local recurrence rate, and is most pronounced in case of low densities of CD4 cells at IM-S regions.

The *CD20 Cluster Score* acts as an independent prognostic marker in early-stage oral-tongue cancer, which emphasizes the biological impact of clustered B-cells and supports their critical role in anti-tumor responses in OSCC.[13,16,20] In various non-OSCC cancers, reports on prognostic values of B-cells are conflicting.[21] In breast, colon, and non-small cell lung cancer, reports have indicated high levels of tumor-associated B-cells

A

Subgroup	*n*	Esimated mean survival (months) CD20 Cluster Score Low	CD20 Cluster Score High	Hazard ratio, 95% CI	Hazard ratio	95% CI	p-value
All patients	138	75.9	99.7		0.377	0.200–0.711	0.003
Stromal CD4							
Low	68	79.7	106.4		0.253	0.084–0.763	0.015
High	70	77.4	77.2		1.386	0.607–3.165	0.438
Stromal CD8							
Low	68	77.0	106.5		0.313	0.117–0.836	0.020
High	70	81.0	89.5		0.671	0.301–1.497	0.330
Stromal CD20							
Low	70	76.5	79.7		1.243	0.550–2.811	0.601
High	68	75.9	107.2		0.175	0.057–0.530	0.002

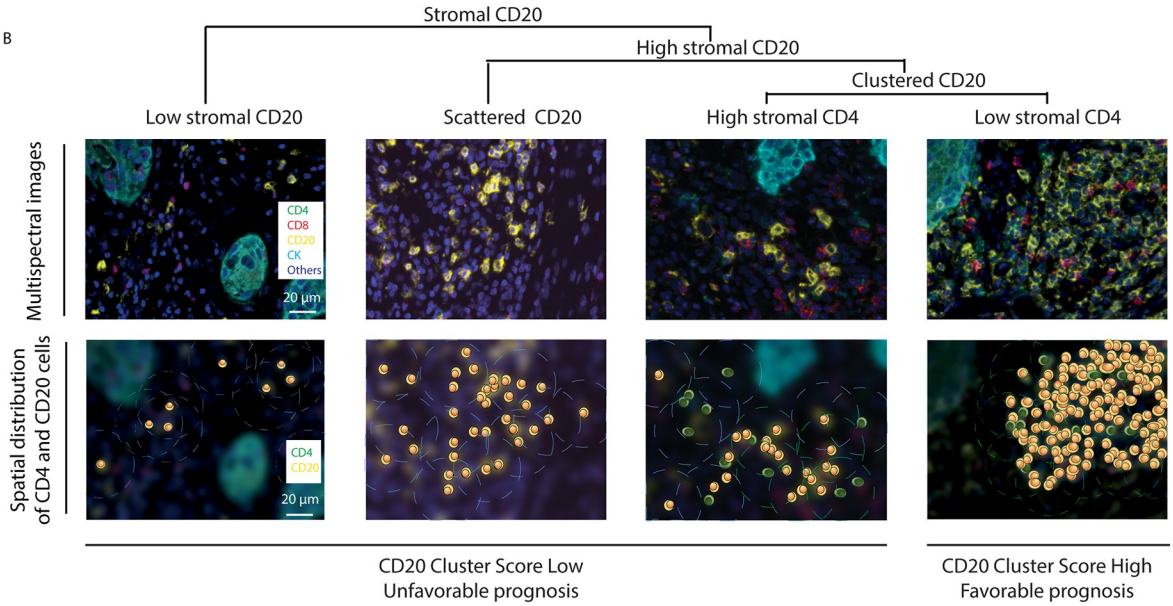

Figure 4. The CD20 cluster score shows dependency on stromal density of CD4 cells. (**A**) *CD20 Cluster Score* subgroup analysis according to stromal density of CD4, CD8 and CD20 cells. (**B**) Scheme of clinically relevant categories of tumors with differential stromal CD20 and CD4 cell densities and CD20 cell clustering. Upper panel shows representative images for each category, and lower panel shows representative overlaid masks of CD4 and CD20.

that related to improved survival.[22–28] However, there are also contradicting reports pointing to tumor infiltrated B-cells and B-cells associated genes in the mentioned cancers that have a negative or no effect on patients' survival.[21,29] This discrepancy may reflect that B-cells may have opposing contributions to anti-tumor immune responses depending on the tumor micro-environment. On the one hand, B-cells may mediate an anti-tumor effect through secretion of antibodies, presentation of tumor antigen to adjacent T-cells, and production of immune-potentiating cytokines, such as IFNγ and IL12.[30–34] On the other hand, B-cells may mediate a pro-tumor effect through induction of neovascularization, becoming regulatory B-cells (Bregs)[35] and production of immune-suppressive cytokines, such as IL10, IL-35, and TGFβ.[36,37] Interestingly, in pancreatic cancer patients, single and scattered CD20 B-cells correlated negatively with survival, whereas non-scattered, organized CD20 B-cells positively correlated with survival.[38] The latter observation probably relates to distinct B-cell aggregates as those that are found in TLS, which are ectopic lymphoid structures that generally support an anti-tumor T-cell response.[39] Recent reports have highlighted the prognostic and predictive value of CD20 and CD4 cells-containing TLS in multiple solid tumors, including cutaneous melanoma,[40] renal cell cancer,[41] sarcoma,[42] breast cancer,[43] non-small cell lung cancer,[44] urothelial cancer,[45] and HNC.[19]

With respect to the inter-relationship between CD20 B-cell clusters and CD4 T-cells, we found a negative correlation between the density of CD4 T-cells and the abundance of CD20 B-cells clusters at IM-S. This observation may imply that high numbers of CD4 T-cells represent regulatory CD4 T-cells (Treg), which are known to suppress TLS formation.[46] In general, HNC is an immunosuppressive tumor type with high numbers of Tregs,[47–49] and it may be that this subset of CD4 T-cells is most abundant in early-stage oral-tongue cancer. High numbers of Treg cells, either alone or in combination with high numbers of CD8 T-cells, associated with better OS.[14,50] We have observed that FOXP3-positive cells make up about 30% of all CD4 T cells (data not shown). How abundance of Tregs relate to *CD20 cluster score* and TLS formation, as well as their relation to prognosis, remains to be tested and is part of our ongoing studies. Besides the abundance of Tregs, we cannot exclude lack of follicular helper CD4 T-cells (Tfh), as this

Table 3. *CD20 Cluster Score* is an independent prognostic parameter for overall survival of early-stage tongue cancer patients.[a]

				Univariate Cox analysis for OS			Multivariate Cox analysis for OS		
Variable		*n*	Estimated mean survival (months)	HR	95% CI	p-value	HR	95% CI	p-value
CD20 Cluster Score	Low	84	75.9						
	High	54	99.7	0.377	0.200–0.711	0.003	0.340	0.177–0.654	0.001
Age	<65	77	100.5						
	≥65	61	72.0	3.284	1.786–6.038	<0.001	4.283	2.252–8.156	<0.001
Gender	Male	78	88.7						
	Female	60	83.9	1.198	0.683–2.102	0.528			
pT	pT1	105	86.9						
	pT2	33	84.7	1.079	0.570–2.043	0.816			
pN	pN	123	86.0						
	pN1	15	93.3	0.683	0.241–1.936	0.474			
pStage	pStage1	101	86.8						
	pStage2&3	37	85.1	1.048	0.561–1.957	0.884			
Differentiation grade	Well & Moderately differentiated	108	86.3						
	Poorly differentiated	27	93.9	0.678	0.303–1.519	0.345			
LVI	Absence	117	87.6						
	Presence	17	81.8	0.722	0.221–2.357	0.590			
PNI	Absence	126	88.6						
	Presence	10	66.4	1.115	0.960–1.296	0.155	1.018	0.868–1.196	0.823
LRR	Non-recurrence	112	90.1						
	Recurrence	26	72.1	1.842	0.988–3.433	0.054	2.479	1.295–4.746	0.006

[a]Table lists univariate and multivariate Cox proportional regression hazards models for OS in the entire cohort (n = 138). Estimated mean survival is shown for each variable. HR, 95% CI and p-value are shown for both univariate and multivariate analysis. Variables giving $p < 0.200$ in univariate analysis were tested in multivariate analysis. Abbreviations: pT, pathological tumor stage; pN, pathological nodal stage; pStage, pathological stage; LVI, lymphovascular invasion; PNI, perineural invasion; LRR, locoregional recurrence.

latter subset of CD4 T-cells is key to germinal center development, and fosters B-cells by providing CD40:CD40L-mediated support of B-cell receptor signaling and cytokine production.[51,52] A recent single-cell RNA-seq together with multiplex staining revealed a highly organized pattern B-cells and Tfh, the occurrence of which translate to longer progression-free survival.[8,53] Future research is required to delineate the exact composition of CD4 T-cell subsets and their relationship with the prognostic value of the *CD20 Cluster Score* in early-stage oral-tongue cancer. Retrospective study design is one of the limitations of our study; however, our findings do provide a clear basis for further prospective studies.

The *CD20 Cluster Score* may provide an easy-to-implement alternative to the detection of TLS, at least in the setting of early-stage tongue cancer. Identification of TLS is challenging in research and clinical implementation due to its complex and ill-defined cellular structure and composition.[54] For example, a variety of single or multiple markers has been used to identify TLS, such as CD20[45], or a combination of CD20, CD21, CD8, CD4 and FOXP3[41]. The more commonly present non-classical TLS in cancers may represent a less organized structure without germinal center formation, which may further impede its correct classification.[19,55–57] It is noteworthy that TLS-related parameters, i.e., presence PNAd-positive HEV, were introduced before in OSCC[19,57] but lack of objective quantification may have limited robustness and clinical implementation. Granted, multiplex IF is not yet widely used in clinical practice, the *CD20 Cluster Score* could be fairly rapidly adapted into a clinical setting as it can be quantified with standard multi-marker (CD4, CD20, CK and nucleus) immunohistochemistry (IHC) per slide, or alternatively with single marker IHC on consecutive slides. It would be of interest to assess the prognostic value of the *CD20 Cluster Score* also in non-OSCC cancers

Besides prognostic value, treatment with immune checkpoint inhibitor (ICI) has been approved for recurrent and metastatic squamous cell carcinoma of HNC and showed higher survival benefit and fewer serious side effects compared to chemotherapy-based treatment.[58,59] Yet, PD-L1 expression status of neither tumor nor immune cells appear to be a robust predictor of treatment efficacy of ICI in advanced HNC (overall response rate 19–23% for ICI monotherapy, and 36–43% for ICI combination therapy).[59] B-cells and TLS-related markers have recently been reported to have predictive value toward response to ICI in the neoadjuvant setting of resectable melanoma and renal cell carcinoma.[41] We argue that the *CD20 Cluster Score* should be part of studies into new predictors for ICI treatment in OSCC.

Taken together, our study defined the *CD20 Cluster Score*, a score that combines two easy-to-measure contextual parameters, captures B-cell clusters in stroma of invasive margin, and has clear prognostic value in early-stage tongue cancer. Future studies are required to test the clinical value of this score in early-stage tongue cancer, particularly in relation to the anti-tumor efficacy of standard or experimental therapies.

Acknowledgments

The authors would like to thank the patients who provide specimens for our research as well as Berdine van de Steen, Esther Oomen, Florence van Lanschot and Kamolwan Gludnim for data collection and technical assistance.

Disclosure statement

The authors declare no potential conflicts of interest.

Funding

No external funding was received for this study

References

1. Bray F, Bray F, Ferlay J, Soerjomataram I, Siegel RL, Torre LA, Jemal A. Global cancer statistics 2018: GLOBOCAN estimates of incidence and mortality worldwide for 36 cancers in 185 countries. CA Cancer J Clin. 2018;68(6):394–424. doi:10.3322/caac.21492.
2. Pfister DG, Pfister DG, Spencer S, Adelstein D, Adkins D, Anzai Y, Brizel DM, Bruce JY, Busse PM, Caudell JJ, Cmelak AJ, et al. Head and neck cancers, version 2.2020, nccn clinical practice guidelines in oncology. J Natl Compr Canc Netw. 2020;18:873–898.
3. Shim SJ, Cha J, Koom WS, Kim GE, Lee CG, Choi EC, Keum KC. Clinical outcomes for T1-2N0-1 oral tongue cancer patients underwent surgery with and without postoperative radiotherapy. Radiat Oncol. 2010;5(1):43. doi:10.1186/1748-717X-5-43.
4. Tam S, Amit M, Zafereo M, Bell D, Weber RS. Depth of invasion as a predictor of nodal disease and survival in patients with oral tongue squamous cell carcinoma.. Head Neck. 2019;41(1):177–184. doi:10.1002/hed.25506.
5. Binnewies M, Roberts EW, Kersten K, Chan V, Fearon DF, Merad M, Coussens LM, Gabrilovich DI, Ostrand-Rosenberg S, Hedrick CC, et al. Understanding the tumor immune microenvironment (TIME) for effective therapy. Nat Med. 2018;24(5):541–550. doi:10.1038/s41591-018-0014-x.
6. Joyce JA, Fearon DT. T cell exclusion, immune privilege, and the tumor microenvironment. Science. 2015;348(6230):74–80. doi:10.1126/science.aaa6204.
7. Hammerl D, Smid M, Timmermans AM, Sleijfer S, Martens JWM, Debets R. Breast cancer genomics and immuno-oncological markers to guide immune therapies. Semin Cancer Biol. 2017;52(Pt 2):178–188. doi:10.1016/j.semcancer.2017.11.003.
8. Bindea G, Mlecnik B, Tosolini M, Kirilovsky A, Waldner M, Obenauf AC, Angell H, Fredriksen T, Lafontaine L, Berger A, et al. Spatiotemporal dynamics of intratumoral immune cells reveal the immune landscape in human cancer. Immunity. 2013;39(4):782–795. doi:10.1016/j.immuni.2013.10.003.
9. Fridman WH, Pages F, Sautes-Fridman C, Galon J. The immune contexture in human tumours: impact on clinical outcome. Nat Rev Cancer. 2012;12(4):298–306. doi:10.1038/nrc3245.
10. Yuen GJ, Demissie E, Pillai S. B lymphocytes and cancer: a love-hate relationship. Trends Cancer. 2016;2(12):747–757. doi:10.1016/j.trecan.2016.10.010.
11. Sharonov GV, Serebrovskaya EO, Yuzhakova DV, Britanova OV, Chudakov DM. B cells, plasma cells and antibody repertoires in the tumour microenvironment. Nat Rev Immunol. 2020;20(5):294–307. doi:10.1038/s41577-019-0257-x.
12. Nelson BH. CD20+ B cells: the other tumor-infiltrating lymphocytes. J Immunol. 2010;185(9):4977–4982. doi:10.4049/jimmunol.1001323.
13. Tsou P, Katayama H, Ostrin EJ, Hanash SM. The emerging role of b cells in tumor immunity. Cancer Res. 2016;76(19):5597–5601. doi:10.1158/0008-5472.CAN-16-0431.
14. de Ruiter EJ, Ooft ML, Devriese LA, Willems SM. The prognostic role of tumor infiltrating T-lymphocytes in squamous cell carcinoma of the head and neck: A systematic review and meta-analysis. Oncoimmunology. 2017;6(11):e1356148. doi:10.1080/2162402X.2017.1356148.
15. Nguyen N, Bellile E, Thomas D, McHugh J, Rozek L, Virani S, Peterson L, Carey TE, Walline H, Moyer J, et al. Tumor infiltrating lymphocytes and survival in patients with head and neck squamous cell carcinoma. Head Neck. 2016;38(7):1074–1084. doi:10.1002/hed.24406.
16. Lao XM, Liang YJ, Su YX, Zhang SE, Zhou XI, Liao GQ. Distribution and significance of interstitial fibrosis and stroma-infiltrating B cells in tongue squamous cell carcinoma. Oncol Lett. 2016;11(3):2027–2034. doi:10.3892/ol.2016.4184.
17. Zhang W, Hubbard A, Jones T, Racolta A, Bhaumik S, Cummins N, Zhang L, Garsha K, Ventura F, Lefever MR, et al. Fully automated 5-plex fluorescent immunohistochemistry with tyramide signal amplification and same species antibodies. Lab Invest. 2017;97(7):873–885. doi:10.1038/labinvest.2017.37.
18. Hadler-Olsen E, Wetting HL, Rikardsen O, Steigen SE, Kanapathippillai P, Grenman R, Winberg JO, Svineng G, Uhlin-Hansen L. Stromal impact on tumor growth and lymphangiogenesis in human carcinoma xenografts. Virchows Arch. 2010;457(6):677–692. doi:10.1007/s00428-010-0980-y.
19. Wirsing AM, Rikardsen OG, Steigen SE, Uhlin-Hansen L, Hadler-Olsen E. Presence of tumour high-endothelial venules is an independent positive prognostic factor and stratifies patients with advanced-stage oral squamous cell carcinoma. Tumour Biol. 2016;37(2):2449–2459. doi:10.1007/s13277-015-4036-4.
20. Wirsing AM, Ervik IK, Seppola M, Uhlin-Hansen L, Steigen SE, Hadler-Olsen E. Presence of high-endothelial venules correlates with a favorable immune microenvironment in oral squamous cell carcinoma. Mod Pathol. 2018;31(6):910–922. doi:10.1038/s41379-018-0019-5.
21. Wouters MCA, Nelson BH. Prognostic significance of tumor-infiltrating b cells and plasma cells in human cancer. Clin Cancer Res. 2018;24(24):6125–6135. doi:10.1158/1078-0432.CCR-18-1481.
22. Al-Shibli KI, Donnem T, Al-Saad S, Persson M, Bremnes RM, Busund LT. Prognostic effect of epithelial and stromal lymphocyte infiltration in non-small cell lung cancer. Clin Cancer Res. 2008;14(16):5220–5227. doi:10.1158/1078-0432.CCR-08-0133.
23. Berntsson J, Nodin B, Eberhard J, Micke P, Jirström K. Prognostic impact of tumour-infiltrating B cells and plasma cells in colorectal cancer. Int J Cancer. 2016;139(5):1129–1139. doi:10.1002/ijc.30138.
24. Brown JR, Wimberly H, Lannin DR, Nixon C, Rimm DL, Bossuyt V. Multiplexed quantitative analysis of CD3, CD8, and CD20 predicts response to neoadjuvant chemotherapy in breast cancer. Clin Cancer Res. 2014;20(23):5995–6005. doi:10.1158/1078-0432.CCR-14-1622.
25. Mahmoud SM, Lee AH, Paish EC, Macmillan RD, Ellis IO, Green AR. The prognostic significance of B lymphocytes in invasive carcinoma of the breast. Breast Cancer Res Treat. 2012;132(2):545–553. doi:10.1007/s10549-011-1620-1.
26. .Mlecnik B, Van den Eynde M, Bindea G, Church SE, Vasaturo A, Fredriksen T, Lafontaine L, Haicheur N, Marliot F, Debetancourt D, et al. Comprehensive intrametastatic immune quantification and major impact of immunoscore on survival. J Natl Cancer Inst. 2018;110(1):97–108. doi:10.1093/jnci/djx123.
27. Schmidt M, Hellwig B, Hammad S, Othman A, Lohr M, Chen Z, Boehm D, Gebhard S, Petry I, Lebrecht A, et al. A comprehensive analysis of human gene expression profiles identifies stromal immunoglobulin κ C as a compatible prognostic marker in human solid tumors. Clin Cancer Res. 2012;18(9):2695–2703. doi:10.1158/1078-0432.CCR-11-2210.
28. Kinoshita T, Muramatsu R, Fujita T, Nagumo H, Sakurai T, Noji S, Takahata E, Yaguchi T, Tsukamoto N, Kudo-Saito C, et al. Prognostic value of tumor-infiltrating lymphocytes differs depending on histological type and smoking habit in completely resected non-small-cell lung cancer. Ann Oncol. 2016;27(11):2117–2123. doi:10.1093/annonc/mdw319.
29. Gentles AJ, Newman AM, Liu CL, Bratman SV, Feng W, Kim D, Nair VS, Xu Y, Khuong A, Hoang CD, et al. The prognostic landscape of genes and infiltrating immune cells across human cancers. Nat Med. 2015;21(8):938–945. doi:10.1038/nm.3909.
30. Hamanaka Y, Suehiro Y, Fukui M, Shikichi K, Imai K, Hinoda Y. Circulating anti-MUC1 IgG antibodies as a favorable prognostic factor for pancreatic cancer. Int J Cancer. 2003;103(1):97–100. doi:10.1002/ijc.10801.
31. Kurtenkov O, Klaamas K, Mensdorff-Pouilly S, Miljukhina L, Shljapnikova L, Chuzmarov V. Humoral immune response to MUC1 and to the Thomsen-Friedenreich (TF) glycotope in patients with gastric cancer: relation to survival. Acta Oncol. 2007;46(3):316–323. doi:10.1080/02841860601055441.

32. Hirasawa Y, Kohno N, Yokoyama A, Kondo K, Hiwada K, Miyake M. Natural autoantibody to MUC1 is a prognostic indicator for non-small cell lung cancer. Am J Respir Crit Care Med. 2000;161(2):589–594. doi:10.1164/ajrccm.161.2.9905028.
33. Bruno TC, Ebner PJ, Moore BL, Squalls OG, Waugh KA, Eruslanov EB, Singhal S, Mitchell JD, Franklin WA, Merrick DT, et al. Antigen-presenting intratumoral b cells affect cd4(+) til phenotypes in non-small cell lung cancer patients. Cancer Immunol Res. 2017;5(10):898–907. doi:10.1158/2326-6066.CIR-17-0075.
34. Deola S, Panelli MC, Maric D, Selleri S, Dmitrieva NI, Voss CY, Klein H, Stroncek D, Wang E, Marincola FM. Helper B cells promote cytotoxic T cell survival and proliferation independently of antigen presentation through CD27/CD70 interactions. J Immunol. 2008;180(3):1362–1372. doi:10.4049/jimmunol.180.3.1362.
35. Zhou X, Su YX, Lao XM, Liang YJ, Liao GQ. CD19(+)IL-10(+) regulatory B cells affect survival of tongue squamous cell carcinoma patients and induce resting CD4(+) T cells to CD4(+)Foxp3(+) regulatory T cells. Oral Oncol. 2016;53:27–35. doi:10.1016/j.oraloncology.2015.11.003.
36. de Visser KE, Korets LV, Coussens LM. De novo carcinogenesis promoted by chronic inflammation is B lymphocyte dependent. Cancer Cell. 2005;7:411–423.
37. Ammirante M, Luo J-L, Grivennikov S, Nedospasov S, Karin M. B-cell-derived lymphotoxin promotes castration-resistant prostate cancer. Nature. 2010;464(7286):302–305. doi:10.1038/nature08782.
38. Castino GF, Cortese N, Capretti G, Serio S, Di Caro G, Mineri R, Magrini E, Grizzi F, Cappello P, Novelli F, et al. Spatial distribution of B cells predicts prognosis in human pancreatic adenocarcinoma. Oncoimmunology. 2016;5(4):e1085147. doi:10.1080/2162402X.2015.1085147.
39. Teillaud JL, Dieu-Nosjean MC. Tertiary lymphoid structures: an anti-tumor school for adaptive immune cells and an antibody factory to fight cancer? Front Immunol. 2017;8:830. doi:10.3389/fimmu.2017.00830.
40. Cabrita R, Lauss M, Sanna A, Donia M, Skaarup Larsen M, Mitra S, Johansson I, Phung B, Harbst K, Vallon-Christersson J, et al. Tertiary lymphoid structures improve immunotherapy and survival in melanoma. Nature. 2020;577(7791):561–565. doi:10.1038/s41586-019-1914-8.
41. Helmink BA, Reddy SM, Gao J, Zhang S, Basar R, Thakur R, Yizhak K, Sade-Feldman M, Blando J, Han G, et al. B cells and tertiary lymphoid structures promote immunotherapy response. Nature. 2020;577(7791):549–555. doi:10.1038/s41586-019-1922-8.
42. Petitprez F, de Reynies A, Keung EZ, Chen TW, Sun CM, Calderaro J, Jeng YM, Hsiao LP, Lacroix L, Bougoüin A, et al. B cells are associated with survival and immunotherapy response in sarcoma. Nature. 2020;577(7791):556–560. doi:10.1038/s41586-019-1906-8.
43. Garaud S, Buisseret L, Solinas C, Gu-Trantien C, de Wind A, Van den Eynden G, Naveaux C, Lodewyckx JN, Boisson A, Duvillier H, et al. Tumor infiltrating B-cells signal functional humoral immune responses in breast cancer. JCI Insight. 2019;5(7791):556–560. doi:10.1172/jci.insight.129641.
44. Silina K, Soltermann A, Attar FM, Casanova R, Uckeley ZM, Thut H, Wandres M, Isajevs S, Cheng P, Curioni-Fontecedro A, et al. Germinal centers determine the prognostic relevance of tertiary lymphoid structures and are impaired by corticosteroids in lung squamous cell carcinoma. Cancer Res. 2018;78(5):1308–1320. doi:10.1158/0008-5472.CAN-17-1987.
45. Goswami S, Chen Y, Anandhan S, Szabo PM, Basu S, Blando JM, Liu W, Zhang J, Natarajan SM, Xiong L, et al. ARID1A mutation plus CXCL13 expression act as combinatorial biomarkers to predict responses to immune checkpoint therapy in mUCC. Sci Transl Med. 2020;12(548):eabc4220. doi:10.1126/scitranslmed.abc4220.
46. Joshi NS, Akama-Garren EH, Lu Y, Lee DY, Chang GP, Li A, DuPage M, Tammela T, Kerper NR, Farago AF, et al. Regulatory T cells in tumor-associated tertiary lymphoid structures suppress anti-tumor t cell responses. Immunity. 2015;43(3):579–590. doi:10.1016/j.immuni.2015.08.006.
47. Whiteside TL. Head and neck carcinoma immunotherapy: facts and hopes. Clin Cancer Res. 2018;24(1):6–13. doi:10.1158/1078-0432.CCR-17-1261.
48. Mandal R, Senbabaoglu Y, Desrichard A, Havel JJ, Dalin MG, Riaz N, Lee KW, Ganly I, Hakimi AA, Chan TA, Morris LGT. The head and neck cancer immune landscape and its immunotherapeutic implications. JCI Insight. 2016;1(17):e89829. doi:10.1172/jci.insight.89829.
49. Hanakawa H, Orita Y, Sato Y, Takeuchi M, Ohno K, Gion Y, Tsukahara K, Tamamura R, Ito T, Nagatsuka H, et al. Regulatory T-cell infiltration in tongue squamous cell carcinoma. Acta Otolaryngol. 2014;134(8):859–864. doi:10.3109/00016489.2014.918279.
50. Watanabe Y, Katou F, Ohtani H, Nakayama T, Yoshie O, Hashimoto K. Tumor-infiltrating lymphocytes, particularly the balance between CD8(+) T cells and CCR4(+) regulatory T cells, affect the survival of patients with oral squamous cell carcinoma. Oral Surg Oral Med Oral Pathol Oral Radiol Endod. 2010;109(5):744–752. doi:10.1016/j.tripleo.2009.12.015.
51. Tangye SG, Ma CS, Brink R, Deenick EK. The good, the bad and the ugly - TFH cells in human health and disease. Nat Rev Immunol. 2013;13(6):412–426. doi:10.1038/nri3447.
52. Turner JS, Ke F, Grigorova IL, Cell Receptor B. Crosslinking augments germinal center b cell selection when t cell help is limiting. Cell Rep. 2018;25(1395–1403):e1394. doi:10.1016/j.celrep.2018.10.042.
53. Cillo AR, Kurten CHL, Tabib T, Qi Z, Onkar S, Wang T, Liu A, Duvvuri U, Kim S, Soose RJ, et al. Immune landscape of viral- and carcinogen-driven head and neck cancer. Immunity. 2020;52(-183–199):e189. doi:10.1016/j.immuni.2019.11.014.
54. Dieu-Nosjean MC, Goc J, Giraldo NA, Sautes-Fridman C, Fridman WH. Tertiary lymphoid structures in cancer and beyond. Trends Immunol. 2014;35(11):571–580. doi:10.1016/j.it.2014.09.006.
55. Engelhard VH, Rodriguez AB, Mauldin IS, Woods AN, Peske JD, Slingluff CL, Jr. immune cell infiltration and tertiary lymphoid structures as determinants of antitumor immunity. J Immunol. 2018;200(2):432–442. doi:10.4049/jimmunol.1701269.
56. Weinstein AM, Storkus WJ. Biosynthesis and functional significance of peripheral node addressin in cancer-associated TLO. Front Immunol. 2016;7:301. doi:10.3389/fimmu.2016.00301.
57. Wirsing AM, Rikardsen OG, Steigen SE, Uhlin-Hansen L, Hadler-Olsen E. Characterisation and prognostic value of tertiary lymphoid structures in oral squamous cell carcinoma. BMC Clin Pathol. 2014;14(1):38. doi:10.1186/1472-6890-14-38.
58. Ferris RL, Blumenschein G, Jr., Fayette J, Guigay J, Colevas AD, Licitra L, Harrington K, Kasper S, Vokes EE, Even C, et al. nivolumab for recurrent squamous-cell carcinoma of the head and neck. N Engl J Med. 2016;375(19):1856–1867. doi:10.1056/NEJMoa1602252.
59. Burtness B, Harrington KJ, Greil R, Soulieres D, Tahara M, de Castro G, Jr., Psyrri A, Basté N, Neupane P, Bratland A,et al. Pembrolizumab alone or with chemotherapy versus cetuximab with chemotherapy for recurrent or metastatic squamous cell carcinoma of the head and neck (KEYNOTE-048): a randomised, open-label, phase 3 study. Lancet. 2019;394(10212):1915–1928. doi:10.1016/S0140-6736(19)32591-7.